

# Observation of timing jitter reduction induced by spectral filtering in a fiber laser mode locked with a carbon nanotube-based saturable absorber

Chunmei Ouyang,<sup>1,\*</sup> Ping Shum,<sup>1</sup> Honghai Wang,<sup>1</sup> Jia Haur Wong,<sup>1</sup> Kan Wu,<sup>1</sup> Songnian Fu,<sup>1</sup>  
Ruoming Li,<sup>1</sup> E. J. R. Kelleher,<sup>2</sup> A. I. Chernov,<sup>3</sup> and E. D. Obraztsova<sup>3</sup>

<sup>1</sup>Network Technology Research Centre, School of Electrical and Electronic Engineering, Nanyang Technological University, 50 Nanyang Drive, Singapore 637553, Singapore

<sup>2</sup>Femtosecond Optics Group, Physics Department, Imperial College London, London SW7 2AZ, UK

<sup>3</sup>A. M. Prokhorov General Physics Institute, Russian Academy of Science, 38 Vavilov Street, Moscow 119991, Russia

\*Corresponding author: cmouyang@ntu.edu.sg

Received April 19, 2010; revised June 11, 2010; accepted June 11, 2010;  
posted June 21, 2010 (Doc. ID 127176); published July 1, 2010

A self-starting passively mode-locked fiber laser with a carbon nanotube-based saturable absorber and a fiber-based bandpass filter (BPF) is proposed. Incorporation of a BPF into the cavity leads to a great reduction of its timing jitter from 84.8 to 29.1 fs (10 Hz–3 MHz). This happens because the filtering effect can weaken the fluctuation of the central wavelength induced by the quantum noise, being one of the important contributions to timing jitter in the optical amplifying process. © 2010 Optical Society of America

OCIS codes: 140.3500, 160.5470, 230.7408, 320.5540.

The timing jitter (or phase noise) characteristic of mode-locked lasers has received considerable attention for its importance in many applications, such as optical clock distribution, optical data transmission, and optical sampling. For mode-locked lasers, the source of timing jitter of pulse trains mainly includes the pump-induced gain fluctuations, the quantum noise from spontaneous emission (SE) in the amplification process, and the cavity length fluctuations. Based on soliton perturbation theory, Haus and Mecozzi [1] proposed an analytical model of timing jitter, which gives physical insight into the role of laser parameters and aids further optimization. Later, it was proven by Paschotta [2,3] that the result of [1] for the timing jitter is still valid for mode-locked lasers not using soliton pulse shaping. They also present a numerical method to evaluate the timing jitter of various mode-locked lasers. Based on the above theory and model, many methods and laser configurations have been proposed to reduce the laser timing jitter. Phase-locked loop (PLL) can minimize the influence of cavity length fluctuations and, thus, suppress the low-frequency timing jitter of actively and passively mode-locked lasers [4,5]. A mode-locked laser with 14.4 fs timing jitter (10 Hz–375 MHz) has been reported with high-bandwidth feedback control on the cavity length and pump power simultaneously [6]. Ozharar *et al.* reduced the timing jitter from 304 to 150 fs (1 Hz–5.12 GHz) by introducing an active intracavity phase modulation [7]. Gee *et al.* generated a residual timing jitter of 380 as (1 Hz–1 MHz) from a mode-locked external-cavity semiconductor laser by optimizing the intracavity dispersion and utilizing a high-power, low-noise InGaAsP quantum-well slab-coupled optical waveguide amplifier gain medium [8]. Jiang *et al.* employed a 0.7 nm bulk bandpass filter (BPF) to reduce the quantum-noise-induced timing jitter in a hybrid mode-locked laser diode and achieved a timing jitter of 47 fs (10 Hz–10 MHz) [9]. More recently, Wu *et al.* reported timing jitter reduction by optimizing the intracavity loss in a carbon nanotube (CNT)-based mode-locked fiber laser [10].

All-fiber mode-locked lasers are highly desired, because the influences on the phase noise from cavity mirror perturbations can be minimized. In this Letter, we experimentally investigate the effect of a fiber-based BPF on the timing jitter in an all-fiber Er-doped mode-locked soliton laser with CNT as a fast saturable absorber. By proper spectral filtering, the timing jitter can be significantly reduced. To our knowledge, it is the first time that a fiber-based filter is applied for achieving low timing jitter in all-fiber passively mode-locked lasers.

The experimental setup is shown in Fig. 1. A 976 nm laser diode was used to pump a 0.5-m-long Er-doped fiber (LIEKKI Er110) with group velocity dispersion (GVD) of 0.012 ps<sup>2</sup>/m through a 980/1550 wavelength division multiplexing (WDM). The length of the single-mode fiber (SMF28) is ~3.7 m with GVD of -0.022 ps<sup>2</sup>/m. The intracavity pigtailed fiber of the WDM is a 1.5-m-long HI1060 fiber with GVD ~ +0.020 ps<sup>2</sup>/m. Thus, the total net cavity

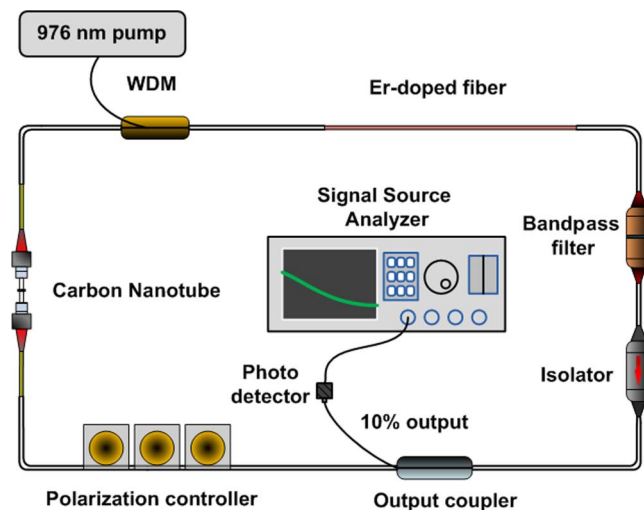


Fig. 1. (Color online) Schematic diagram of an Er-doped mode-locked all-fiber laser with a carbon nanotube composite as a fast saturable absorber.

dispersion is  $\sim -0.045 \text{ ps}^2/\text{m}$  at 1550 nm. The total cavity length is  $\sim 5.7 \text{ m}$ , corresponding to the fundamental repetition rate of  $\sim 36.6 \text{ MHz}$ . An optical isolator was incorporated into the ring cavity to keep the unidirectional operation of the laser. A 10% output coupler extracts the pulse from the cavity. A single-walled CNT-contained composite is used as a saturable absorber for self-starting mode-locking operation. The individual CNTs are distributed in a carboxymethyl cellulose (CMC) film and allow a high damage threshold and low self-starting pump power [11,12]. The CNT-based mode-locker is fabricated by placing the CNT composite between the fiber ends of two FC/PC connectors, as shown in Fig. 1. A fiber-based PC was also included to adjust the pulse polarization. A commercially available fiber-based film BPF was employed, with bandwidth of 16.8 nm at the central wavelength of 1551 nm. The timing jitter of the output signal was characterized with a signal-source analyzer (SSA, Rohde and Schwarz FSUP26), and the power spectral density of the phase noise could be measured.

To get insight into the effects of the spectral filtering on the timing jitter of the soliton pulse trains, we compare the output characteristics with and without the BPF in the cavity. When the pump power is above 40 mW, the laser always self starts without adjusting the PC. Figure 2 gives the autocorrelation traces and the spectral profiles of the output pulses. It is clearly seen that the output pulse characteristics are changed by the existence of the BPF. Without intracavity BPF, typical spectrum (dashed line) with soliton sidebands, a 3 dB bandwidth of  $\sim 6.8 \text{ nm}$  and central wavelength at 1564 nm, can be observed in Fig. 2(a). When the BPF is employed, the sideband structures are removed and the central wavelength shifts to 1557 nm with a bandwidth of 1.6 nm. The spectrum has an asymmetric pedestal at the short wavelength side due to the filtering effect of the BPF, as shown in Fig. 2(a). As for the temporal waveform, Fig. 2(b) shows that the output pulse duration is 1.10 ps and 218 fs (assuming sech<sup>2</sup> profiles), respectively, for the cavity with and without the BPF. Thus, the corresponding time–bandwidth products are 0.382 and 0.320, implying nearly transform-limited pulses.

Next, we measure the timing jitter of our laser in these two cases using the SSA. The phase noise at the 12th harmonic ( $\sim 439 \text{ MHz}$ ) is measured and the timing jitter is integrated from 10 Hz to 3 MHz, as shown in Fig. 3(a). Obviously, the phase noise is reduced at high frequency offset when the spectral filtering is imposed in the laser. The timing jitter (10 Hz–3 MHz) is reduced significantly by

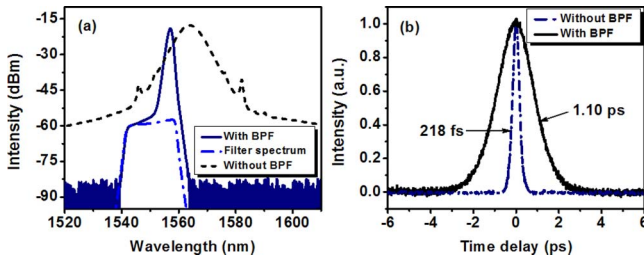


Fig. 2. (Color online) Temporal and spectral profiles of the output pulse with BPF and without BPF in the cavity: (a) optical spectra of output pulses and the transmission spectrum of the BPF; (b) autocorrelation traces of output pulses.

66% from 84.8 to 29.1 fs due to the intracavity BPF. The RF spectrum of the output pulses with BPF inside the cavity is shown in Fig. 3(b), which clearly demonstrates a stable mode-locking of our laser, with a signal-to-noise ratio up to 90 dB at a resolution bandwidth of 300 Hz. Moreover, no sidebands within a wide frequency range were observed, which further suggests that a highly stable mode locking was obtained in the laser.

According to Haus' model, noise sources contributing to the timing jitter of pulse trains include classical noise sources, such as pump power fluctuations and laser cavity length perturbations, and quantum noise arising from the SE in the gain medium. Classical noise can be significantly weakened by using good pump sources and all-fiber structured laser cavities, as well as the PLL technique, in which case quantum noise will dominate the timing jitter generation. The complete expression for the timing jitter spectrum induced by spontaneous emission noise (quantum noise) can be given by [1]

$$S_t(f) = \frac{4D^2}{T_{rt}^2} \frac{D_p}{(2\pi f)^2((2\pi f)^2 + \tau_p^{-2})} + \frac{D_t}{(2\pi f)^2}, \quad (1)$$

where  $D_p = 2/(3\omega_0\tau^2)\theta(2g/T_{rt})h\nu$  and  $D_t = \pi^2\tau^2/(6\omega_0)\theta(2g/T_{rt})h\nu$  are diffusion constants of quantum noise, representing the noise properties of offset frequency and timing, respectively,  $\theta$  is the enhancement factor due to the incomplete inversion of the gain medium,  $\tau_p = (3\pi^2 T_{rt} \Delta f_g^2 \tau^2)/(2g)$  is the relaxation time,  $D$  is half of the total GVD,  $T_{rt}$  is the round-trip time,  $\omega_0$  is the pulse energy in the cavity,  $\tau$  is the pulse duration,  $g$  is the incremental gain per round trip, and  $\Delta f_g$  is the gain bandwidth.

The first term in Eq. (1) indicates an indirect effect of SE noise on the timing jitter by causing the fluctuations of the pulse central frequency, which can couple to the timing jitter through intracavity dispersion. The second term shows a direct effect, leading to  $S_t(f) \propto f^{-2}$ . In the high-frequency region, the first term decreases by a factor of  $f^{-4}$  and, in the low-frequency region, it decreases by  $f^{-2}$ . When the finite gain spectrum providing a restoring force is included, the fluctuations of the central frequency can be modified. When the gain bandwidth  $\Delta f_g$  decreases, this restoring force is enhanced. Thus, the timing jitter from the first term is reduced, which will lead to the reduction of the total timing jitter. However, this trend is not monotonic. As the gain bandwidth is further narrowed, the generated pulse is much stretched in time domain because of the small pulse bandwidth. Thus, the first term becomes smaller, while the second term becomes larger, finally

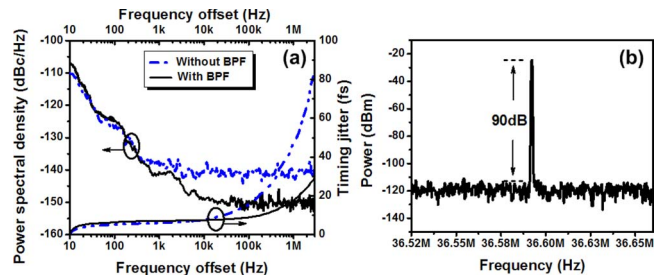


Fig. 3. (Color online) (a) Phase-noise power spectral density and integrated timing jitter with and without BPF. (b) RF spectrum of the output pulse with BPF inside the cavity.

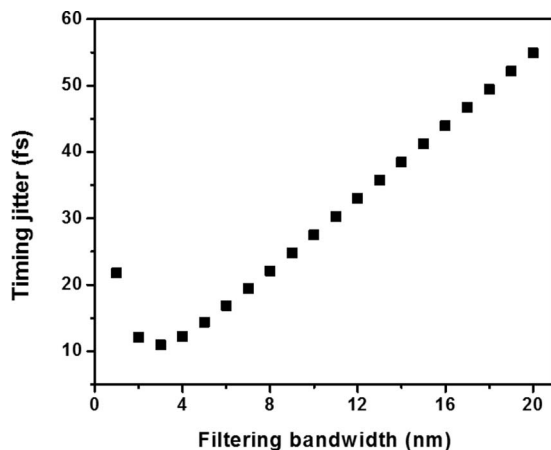


Fig. 4. (Color online) Dependence of the timing jitter on the filtering bandwidth in a mode-locked fiber laser, obtained by analytical calculation with parameters of our laser.

resulting in the increase of the timing jitter. Using the parameters of our laser, we calculate the variance of the timing jitter with filtering bandwidth, as shown in Fig. 4. The values are slightly smaller than the ones obtained in the experiment because the pump fluctuations and laser cavity perturbations make a contribution to the timing jitter experimentally. Thus, by properly selecting the filtering bandwidth in lasers, the timing jitter obtained can be minimized.

In the experiment, we used an available fiber-based BPF to limit the timing jitter induced by central frequency fluctuations. Because the filtering bandwidth of the BPF is wide, and therefore the restoring force is weak, we choose an appropriate gain fiber length that results in a 1564 nm gain peak. Thus coactivation of the effective gain bandwidth and the BPF with the central wavelength of 1551 nm realizes an effective narrow-filtering bandwidth, which is near the optimized bandwidth as shown in Fig. 4. The restoring force, induced by the effective filter, largely reduced the timing jitter contributed by the quantum noise. For the resultant pulse stretching, the second term in Eq. (1) tends to become larger, while the first term tends to become smaller due to the small pulse bandwidth, so that the influence on the total timing jitter is weak. Additionally, the central frequency shifts to the short wavelength due to the BPF, which will make the net cavity dispersion decrease to further reduce the timing jitter.

The use of CNTs as the saturable absorber for mode locking also allows us to obtain low timing jitter. The CNTs have a recovery time of less than 300 fs [13], so it acts as a fast saturable absorber and will not contribute to the timing jitter of the pulse trains compared with slow saturable absorbers [2,3].

In conclusion, we have experimentally observed that the timing jitter of a fiber laser passively mode-locked with a CNT-based saturable absorber was reduced from 84.8 to 29.1 fs (10 Hz–3 MHz) using a fixed fiber-based BPF within the laser cavity. Detailed comparisons were made between the laser performance with and without the BPF in the cavity. Furthermore, we presented the theoretical analysis of the experimental results based on Haus' model and gave the dependence of the timing jitter on the filtering bandwidth. We conclude that the filtering of the BPF introduces a restoring force to limit the central wavelength perturbations induced by quantum noise that will contribute to the timing jitter of the pulses.

## References

1. H. A. Haus and A. Mecozzi, *IEEE J. Quantum Electron.* **29**, 983 (1993).
2. R. Paschotta, *Appl. Phys. B* **79**, 153 (2004).
3. R. Paschotta, *Appl. Phys. B* **79**, 163 (2004).
4. C. M. Depriest, T. Yilmaz, A. Braun, J. Abeles, and P. J. Delfyett, *IEEE J. Quantum Electron.* **38**, 380 (2002).
5. S. Masuda, S. Niki, and M. Nakazawa, *Opt. Express* **17**, 6613 (2009).
6. J. B. Schlager, B. E. Callicoatt, R. P. Mirin, and N. A. Sanford, *Opt. Lett.* **28**, 2411 (2003).
7. S. Ozharar, I. Ozdur, F. Quinlan, and P. J. Delfyett, *Opt. Lett.* **34**, 677 (2009).
8. S. Gee, S. Ozharar, J. J. Plant, P. W. Juodawlkis, and P. J. Delfyett, *Opt. Lett.* **34**, 238 (2009).
9. L. A. Jiang, M. E. Grein, and E. P. Ippen, *Opt. Lett.* **27**, 49 (2002).
10. K. Wu, J. H. Wong, P. Shum, D. R. C. S. Lim, V. K. H. Wong, K. E. K. Lee, J. P. Chen, and E. D. Obraztsova, *Opt. Lett.* **35**, 1085 (2010).
11. A. V. Tausenev, E. D. Obraztsova, A. S. Lobach, A. I. Chernov, V. I. Konov, P. G. Kryukov, A. V. Konyashchenko, and E. M. Dianov, *Appl. Phys. Lett.* **92**, 171113 (2008).
12. A. I. Chernov, E. D. Obraztsova, and A. S. Lobach, *Phys. Status Solidi B* **244**, 4231 (2007).
13. P. A. Obraztsov, A. A. Sirotkin, E. D. Obraztsova, Yu. P. Svirko, and S. V. Garnov, *Opt. Rev.* **17**, 290–293 (2010).